

Witnessing mass-energy equivalence with trapped atom interferometers

Jerzy Paczos¹, Joshua Foo^{2,3,4}, and Magdalena Zych^{1,5}

¹Department of Physics, Stockholm University, SE-106 91 Stockholm, Sweden

²Centre for Quantum Computation and Communication Technology, School of Mathematics and Physics, University of Queensland, St. Lucia, Queensland 4072, Australia

³Department of Physics, Stevens Institute of Technology, Castle Point Terrace, Hoboken, New Jersey 07030, USA

⁴Department of Physics and Astronomy, University of Waterloo, Waterloo, Ontario, Canada, N2L 3G1

⁵Centre for Engineered Quantum Systems, School of Mathematics and Physics, The University of Queensland, St. Lucia, Queensland, 4072, Australia

We propose an experimental setup to probe the interplay between the quantum superposition principle and gravitational time dilation arising from the mass-energy equivalence. It capitalizes on state-of-the-art atom interferometers that can keep atoms trapped in a superposition of heights in Earth’s gravitational field for exceedingly long times, reaching the minute scale. Our proposal consists of adding two additional laser pulses to the existing experiments that would set up a clock trapped at a superposition of heights, reading a quantum superposition of relativistic proper times. We develop a method to include relativistic corrections to Bloch oscillations, which describe the trapped part of the interferometer. We derive the trajectories and corresponding phases acquired in each arm of the interferometer. We then show that a superposition of proper times manifests in the interference pattern in two ways: visibility modulations and a shift of the atom’s resonant frequency. We argue that the latter might be observable with current technology.

—*Introduction.* A key prediction of general relativity is that time is not a global background parameter but flows at different rates depending on the spacetime geometry, a phenomenon known as time dilation [1]. The physical effects pro-

duced by time dilation have been tested in numerous paradigmatic experiments: Pound and Rebka were the first to observe an altitude-dependent gravitational redshift in gamma rays emitted between the top and bottom of a tower [2]; Hafele and Keating directly tested special and general relativistic time dilation by comparing atomic clocks at different heights and moving at different speeds [3]; and Shapiro proposed to measure the reduction in the speed of light for electromagnetic waves traveling across regions subject to a gravitational potential [4], an effect later observed in [5]. These effects are fully explainable in classical relativistic physics.

The first experiment to measure the effect of gravity on the quantum wavefunction of a single particle was performed by Colella, Overhauser, and Werner (COW) [6]. In this setup, neutrons travel in a superposition of heights in Earth’s gravitational field, following the geometry of a Mach-Zehnder-type interferometer. The neutrons, traversing arms at different heights in the gravitational potential, acquire a relative phase. The resulting interference pattern was measured, yielding a phase shift consistent with Earth’s gravitational potential. These experiments, and related measurements with atoms [7–22], thus test non-relativistic gravitational effects in quantum systems.

The proposal to unambiguously probe the interplay between quantum mechanics and general relativity was developed in [23, 24]. These works considered interferometric experiments with particles having an internal degree of freedom that can be treated operationally as a “quantum clock”. The internal evolution would then de-

Jerzy Paczos: jerzy.paczos@fysik.su.se

Joshua Foo: jfoo@stevens.edu

Magdalena Zych: magdalena.zych@fysik.su.se

pend on the proper time along the paths taken through curved spacetime [23–34]. Specifically, the authors of [24] predicted that the experiment would exhibit oscillations in the interference visibility — defined as the contrast between constructive and destructive fringes — which, in non-relativistic COW-type treatments, is always maximal in principle. The predicted periodic modulations of the visibility would be an effect that arises unambiguously from the interplay between relativistic and quantum physics. Several proposals have been made to investigate this effect in interferometric experiments with electrons [35], and with atoms [27, 28, 36–38]. However, given the size of the interferometer required for a reasonable visibility drop [24], it is rather unlikely that this effect will be observed in the near future.

Derivations of the dynamics of relativistic quantum particles with quantized internal mass-energy — necessary for predicting the above experiments — have been performed both within relativistic quantum mechanics [39–42] and via quantum field theory on curved backgrounds [28, 43, 44]. In the low-energy limit for the center-of-mass motion of the composite particles, these two approaches coincide. These results have been applied to model particle dynamics in clock interferometers [27, 28, 35–37, 45] and in trapped-particle setups [46, 47]. In particular, they have been used in optical-clock studies to explore relativistic contributions to the clock’s frequency and precision in [48–50], and, most recently, to explore associated many-body effects [51].

In this work, we propose a concrete experimental setup for witnessing time dilation effects in atom interferometry. Our idea is inspired by the rapid development of trapped atom interferometers [18–22] utilizing Bloch oscillations to keep atoms in a coherent superposition of heights in a gravitational field for increasingly long times, reaching the minute scale [22]. We propose a modification of the existing interferometers by adding two “clock pulses” at the beginning and end of the Bloch oscillations, effectively placing a clock in a superposition of heights and thus of proper times. We develop a method to include relativistic mass–energy corrections in the Bloch oscillations and use it to derive all phases acquired along the interferometer trajectories. We then analyze the resulting interference pattern. We recover the visibility modulations predicted

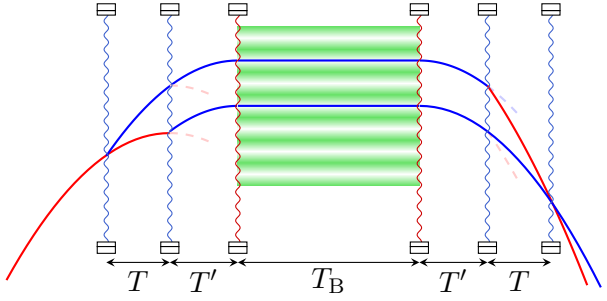


Figure 1: Proposed setup. All motion is restricted to one dimension (parallel to the gravitational field). Blue wavy lines represent $\pi/2$ Bragg pulses splitting the trajectory of the atom, while red wavy lines represent the $\pi/2$ clock pulses affecting only the internal state of the atom. The optical lattice (green striped pattern) is turned on exactly when the blue trajectories reach their apex and off after time T_B . Shaded dashed lines represent trajectories lost within the interferometer.

in [24], which assumed fixed classical trajectories of the clocks, and crucially predict a clock frequency shift that renders this proposal experimentally feasible.

Indeed, the proposed setup implements Ramsey spectroscopy for spatially superposed atoms, allowing for measurements of their resonant frequencies. We show that relativistic effects manifest therein as resonant-frequency shifts. We argue that this will be easier to observe than the visibility oscillations thanks to the extreme precision of frequency measurements [52, 53]. For the height separations reported in ref. [20], the predicted fractional frequency shift is of order 10^{-22} — one order of magnitude smaller than current experimental precision. By revealing effects potentially detectable with existing technology, our proposal represents a major step toward experimental tests of the interplay between quantum mechanics and general relativity.

—*Setup.* Let us consider a one-dimensional atom interferometry setup, Fig. 1, closely resembling configurations implemented in [18–22]. It involves highly cooled atoms¹ moving along the gravitational field g , with their velocity manipulated by Bragg pulses and an optical lattice. We assume that atoms have a two-level internal structure, with ground and excited states separated by energy $\hbar\omega_0$.

Atoms are prepared in their ground state and

¹In experiments [20–22], the temperature reaches a few hundred nanokelvins.

launched upward with initial velocity v_0 , entering free fall under gravity. Then, two $\pi/2$ Bragg pulses are applied, separated by an interval T . Each pulse splits the atomic trajectory into two: one retains its velocity, while the other is shifted by Δv . Consequently, each initial trajectory splits into four paths with two distinct velocities: two with $v_0 - gT$ and two with $v_0 - gT + \Delta v$. We focus on the latter two paths, assuming that the others are lost, as in [18–22].

When the relevant trajectories reach their apex at time $T + T' = (v_0 + \Delta v)/g$, the optical lattice is switched on, and atoms perform Bloch oscillations. When the lattice is switched on, we introduce our modification—a clock pulse at frequency ω that places atoms into an equal superposition of the two internal states without affecting their momentum [54–60]. The optical lattice remains on for a duration T_B , after which the second clock pulse is applied and the lattice is turned

off. The atoms then fall freely for time T' , after which another pair of $\pi/2$ Bragg pulses (separated by an interval T) is applied to recombine the trajectories. At this stage, two additional trajectories are lost, unlike in [18–22], where all output ports are measured, although only two interfere (a simplification introduced here for clarity in the subsequent analysis).

In the end, one measures the probabilities $P_g^{(j)}$ that the atoms are found in the ground state in output trajectory $j \in \{0, 1\}$ (with 0 and 1 corresponding to the red and blue trajectories in Fig. 1, respectively). Apart from the non-relativistic phase $\Delta\phi$ between the upper and lower ground-state trajectories (measured in typical interferometric experiments, e.g. [20]), there will be additional phases δ_d and δ_u acquired within the optical lattice by the excited state on the lower and upper trajectories and which can be measured with the proposed setup. The probability $P_g^{(j)}$ is given by (see Appendix A for derivation):

$$P_g^{(j)} = \frac{1}{16} \left[1 - \cos\left(\frac{\delta_u + \delta_d}{2}\right) \cos\left(\frac{\delta_u - \delta_d}{2}\right) + 2(-1)^j \cos\left(\Delta\phi + \frac{\delta_u - \delta_d}{2}\right) \sin\left(\frac{\delta_d}{2}\right) \sin\left(\frac{\delta_u}{2}\right) \right]. \quad (1)$$

To eliminate the $\Delta\phi$ -dependence, we calculate the total probability $P_g = P_g^{(0)} + P_g^{(1)}$ of finding the atom in the ground state

$$P_g = \frac{1}{8} \left[1 - \cos\left(\frac{\delta_u - \delta_d}{2}\right) \cos\left(\frac{\delta_u + \delta_d}{2}\right) \right]. \quad (2)$$

This probability depends only on the evolution confined to the optical-lattice region, where the atom effectively behaves as a clock in a superposition of heights. The presence of two clock pulses is the sole modification to previous implementations [18–22]. Note that without these pulses, the ground-state probability would remain fixed at 1/4 (recall that we lose some of the trajectories). In our setup, they oscillate between 0 and 1/4 as a function of the time T_B between the clock pulses.

—*Dynamics and phases.* We now analyze the optical-lattice stage of the interferometer and the additional phases δ_d and δ_u acquired by the excited state. During this stage, the atom undergoes Bloch oscillations in a superposition of two heights separated by Δz . We adopt a simplified model of Bloch oscillations (see [19, 61] and Fig. 2), in which the atom interacts with the

optical lattice only when its downward velocity reaches $v_B = \hbar k/m$ (here k is the wave vector of the optical-lattice laser and m is the mass of the ground-state atom). At that point, the atom instantaneously exchanges two photons with the lattice. For an appropriately chosen lattice-light frequency, this leads to velocity reversal occurring always at the same height, causing the atom to oscillate with period $\tau_B = 2v_B/g$. We will assume that the laser frequency has been chosen exactly this way. Each oscillation thus begins and ends at the apex of a free-fall trajectory. Over the hold time T_B , the atom completes N full oscillations, with the final one possibly extended or shortened by an additional time $\tau \in (-\tau_B/2, \tau_B/2)$, reflecting that T_B need not be an integer multiple of τ_B .

Crucially, due to the mass difference between the excited and ground states of the atom, the condition for oscillations at the fixed height can be satisfied only for one internal state at a time for a given lattice frequency. If the lattice is tuned to satisfy this condition for the ground state, the excited state will fall below the starting height after each oscillation. However, as shown in Ap-

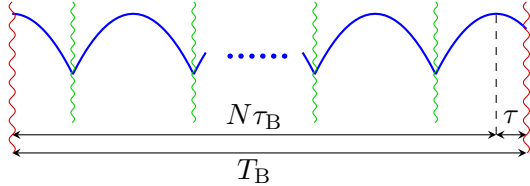


Figure 2: Trajectory followed by the atom (at the lower or upper trajectory) in the optical lattice. We adopt a simplified model of Bloch oscillations in which the atom follows a bouncing trajectory at a fixed height. The total time of Bloch oscillations T_B need not be equal to an integer multiple of Bloch periods $N\tau_B$. Instead, $T_B = N\tau_B + \tau$ with $\tau \in (-\tau_B/2, \tau_B/2)$.

pendix B, in viable experimental scenarios, the cumulative fall distance is much smaller than the atom's thermal de Broglie wavelength. Therefore, the perturbative approach of [62] is justified, allowing us to approximate that both internal states follow the same trajectory. This approximation is further validated in Appendix D.

The phases δ_d and δ_u comprise two contributions: the laser phase ωT_B acquired by the excited state due to the clock pulses, and a propagation-phase correction arising from the different masses of the ground and excited states. To calculate the latter, we follow [62] and write the excited-state Lagrangian as $L_e = L_g + \delta L$, where L_g is the ground-state Lagrangian and δL is a small correction resulting from the rest-mass difference between the two states. If we denote this mass difference by $\delta m = \hbar\omega_0/c^2$, the Lagrangian correction is given by:

$$\delta L = -\delta m \left(c^2 + gz - v^2/2 \right). \quad (3)$$

To calculate the propagation-phase correction, we integrate δL along the atom's trajectory and divide by \hbar . The full derivation is given in Appendix C; a non-perturbative calculation is presented in Appendix D. This yields the expressions for the phases δ_d and δ_u :

$$\begin{aligned} \delta_d &= \left[\omega - \omega_0 \left(1 - \frac{\langle v^2 \rangle}{2c^2} \right) \right] T_B, \\ \delta_u &= \left[\omega - \omega_0 \left(1 - \frac{\langle v^2 \rangle}{2c^2} + \frac{g\Delta z}{c^2} \right) \right] T_B, \end{aligned} \quad (4)$$

where $\langle v^2 \rangle = v_B^2/3$ is the mean square speed within a single oscillation.

In principle, mass–energy corrections to the interferometric phases are not the only $\mathcal{O}(1/c^2)$ ef-

fects present in our proposed experiment. Following Werner et al. [63], one could also include higher-order corrections from the expansion of the free-fall Lagrangian of the relativistic particle, and $\mathcal{O}(1/c^2)$ corrections to the laser phases arising from elastic interactions (Bragg and Bloch pulses). Because these contributions depend only on the atomic trajectory, and since we approximate that both internal states follow the same path, they modify only the interferometric phase $\Delta\phi$, leaving δ_d and δ_u unmodified. However, $\mathcal{O}(1/c^2)$ corrections to $\Delta\phi$ lie beyond the main focus of this work and will be neglected.

Conversely, any corrections to the clock-pulse phases would affect δ_d and δ_u if present. Note that the laser-phase corrections calculated in [63] arise from assuming resonant atom-light interactions, with the atom interacting with photons whose laboratory-frame frequencies depend on its position and velocity. Here, we instead assume the clock pulses operate at a fixed laboratory-frame frequency, permitting non-resonant processes. Under this assumption, there are no corrections to the clock-pulse phases, since the atom interacts with photons at the same frequency regardless of its height or velocity.

—Results and discussion. Let us introduce $\varepsilon_k = \langle v^2 \rangle / 2c^2$ for the kinetic correction in Eq. (4) and $\varepsilon_g = g\Delta z / c^2$ for the gravitational correction. Denoting the quantum-mechanical mean internal frequency by $\langle \omega_0 \rangle = \omega_0 (1 - \varepsilon_k + \varepsilon_g/2)$, the ground-state detection probability (cf. Eq. (2)) can be written as:

$$P_g = \frac{1}{8} [1 - \mathcal{V}(T_B) \cos((\omega - \langle \omega_0 \rangle) T_B)], \quad (5)$$

where $\mathcal{V}(T_B) := \cos(\varepsilon_g \omega_0 T_B / 2)$ is the interferometric visibility. In a generic operating regime away from resonance, the visibility envelope varies slowly with time T_B compared to the rapid oscillations of $\cos((\omega - \langle \omega_0 \rangle) T_B)$. Thus, Eq. (5) yields an interference pattern comprising fast oscillations modulated by a slowly varying envelope. Apart from the visibility modulations, Eq. (5) looks like a result of a Ramsey interferometry experiment for an atom with internal transition frequency $\langle \omega_0 \rangle$. For a fixed T_B , scanning the clock-pulse frequency ω reveals the resonance at $\omega = \langle \omega_0 \rangle$. Consequently, relativistic effects arising from mass–energy equivalence can be probed in two ways: by observing visibility oscillations, and by measuring the resulting

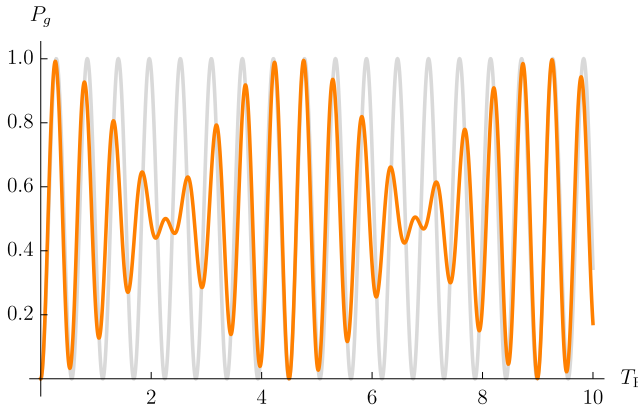


Figure 3: Oscillations of the (normalized) probability P_g for exemplary values $\omega = 40\pi$, $\omega_0 = 1.1\omega$, and $\varepsilon_k = 0.01$, and two different values of the gravitational correction: $\varepsilon_g = 0$ (in gray) and $\varepsilon_g = \varepsilon_k$ (in orange). Note that, apart from visibility modulations, the orange pattern has its frequency shifted against the gray one.

fractional frequency shift

$$\left\langle \frac{\delta\omega_0}{\omega_0} \right\rangle \equiv \frac{\langle \omega_0 \rangle - \omega_0}{\omega_0} = -\varepsilon_k + \frac{\varepsilon_g}{2}. \quad (6)$$

Note that whereas visibility oscillations are sensitive only to the gravitational correction ε_g , the frequency shift depends on both ε_g and ε_k . To distinguish the gravitational and kinetic contributions in fractional-frequency-shift measurements, one can modulate the height separation Δz , which alters ε_g but not ε_k . The probability P_g as a function of time is shown in Fig. 3 for exemplary values of ω , ω_0 , ε_g , and ε_k .

Assuming the experimental parameters as in [20], we would have the velocity $v_B \sim 10$ mm/s, and the vertical separation of the trajectories $\Delta z \sim 10$ μm . This would mean that the corrections would be of the order $|\varepsilon_k| \sim |\varepsilon_g| \sim 10^{-22}$. The fractional frequency shift of that order is very close to what can be currently detected [52, 53, 64, 65]. Indeed, state-of-the-art atomic clocks reach the multiple-measurement precision of the order of 10^{-21} [52, 53, 65] (the lowest single-measurement precision in such experiments is $\sim 10^{-19}$ [66]), which is the order of magnitude for the fractional frequency shift in the proposed experiment for separations $\Delta z \sim 100$ μm , which has already been achieved in [20], at the expense of shorter coherence time.

On the other hand, for a transition frequency $\omega_0 \sim 10^{15}$ Hz and a lattice-hold time $T_B \sim 1$ s (as in [20]), with $|\varepsilon_g| \sim 10^{-22}$, the predicted visibility drop is of order 10^{-15} . This is far below

current experimental sensitivity. Although strontium atoms can support coherent Bloch oscillations for over 100 s [67], the longest achieved to date is ~ 1 s. Minute-scale oscillation times have been demonstrated with cesium atoms [21, 22], but their lower ω_0 renders the effect even weaker. Extending T_B to 100 s would amplify the visibility oscillations by 10^4 , yet they would remain negligible. To achieve an observable visibility drop (of order $0.01 - 1$), one would need a trajectory separation of $\Delta z \sim 10 - 100$ cm. Such separations exceed current capabilities and would likely require two independent lattice lasers.

Note that the observation of the frequency shift (6) itself would not be evidence of the quantum clock reading the superposition of proper times, since the frequency shift is the same as for the clock being in a statistical mixture of two heights. To reject the latter possibility, one can, apart from the total probability P_g of measuring the atom in the ground state at the output, extract from the measured data also the difference $D_g \equiv P_g^{(0)} - P_g^{(1)}$ given by (compare with Eq. (1))

$$D_g = \frac{1}{8} \cos\left(\Delta\phi + \frac{\delta_u - \delta_d}{2}\right) \sin\left(\frac{\delta_d}{2}\right) \sin\left(\frac{\delta_u}{2}\right), \quad (7)$$

where δ_d and δ_u are given in Eq. (4), and $\Delta\phi$ reads (see Appendix C for derivation)

$$\Delta\phi = -\frac{mg\Delta z}{\hbar} (T + 2T' + \tau). \quad (8)$$

If the atom is in a superposition of heights, D_g will oscillate with time T_B . On the other hand, for the atom following a statistical mixture of two heights, the probability difference would be equal to zero. Therefore, extracting from the interferometric output the fractional frequency shift and the oscillations of D_g would provide evidence that the atom was reading a superposition of proper times.

It is important to emphasize that the method proposed in this work does not rely on the assumption that the ground and excited states follow the same trajectories within the optical lattice. While we showed that, within the required order $1/c^2$ of calculating the phases acquired in the interferometer, the trajectories associated with different mass-energy states can be approximated as equal, the method allows accounting for mass-energy corrections and the resulting phases beyond this approximation. Furthermore, we emphasize that our results do not depend crucially

on the simplified Bloch oscillation model we have adopted. Indeed, in Appendix E, we derive analogous results using the usual description of Bloch oscillations [68, 69], in which the atom oscillates under a periodic potential of the optical lattice.

The assumption of zero momentum transfer from the clock pulse is well motivated in special cases, including the usual Lamb-Dicke regime of optical-lattice traps [54, 56–58], and is exact in the case of two-photon E1-M1 clock transitions [55, 59, 60]. The Lamb-Dicke regime is reached when the atomic motion is limited to a region smaller than the transition wavelength. It was shown [54] that in this case, most transitions occur at the internal transition frequency and do not alter the center-of-mass motion of the atom. However, such behavior is well understood only in the fully quantum picture (with quantized center-of-mass motion) — in our simplified picture with the atom following a semiclassical trajectory, the no-recoil assumption is made as a simplifying yet justified approximation. By contrast, for E1-M1 transitions [55, 59, 60], involving two counter-propagating photons with equal frequencies, the clock transition is recoilless as a rule. In this case, the no-recoil assumption is also well motivated in our simplified model of Bloch oscillations.

Abandoning the assumption of zero momentum transfer naturally leads to recoil shifts [70, 71]. In our model, this implies that the ground and excited states follow different trajectories, and the description becomes significantly more involved. The analysis of this case goes beyond the scope of the present work.

Note that the interpretation of the experiment as spectroscopy of a clock in a superposition of heights is possible only by including the laser phases and the explicit mechanism that establishes the quantum clock. These elements were absent in the idealized scenarios of [23, 24] and in the recent proposal using optical tweezers [38]. Consequently, the possibility of measuring the relativistic frequency shift in such interferometric setups has gone unnoticed until now.

Acknowledgments

We thank Timothy Le Pers, Navdeep Arya, Germain Tobar, Jun Ye, Kyungtae Kim, and Charles Baynham for helpful discussions and useful comments. The authors acknowledge the Knut and

Alice Wallenberg Foundation through a Wallenberg Academy Fellowship No. 2021.0119. J.F. acknowledges funding from the U.S. Department of Energy, Office of Science, ASCR under Award Number DE-SC0023291 and Australian Research Council Centre of Excellence for Quantum Computation and Communication Technology (No. CE1701000012).

References

- [1] A. Einstein. “Zur elektrodynamik bewegter körper”. *Annalen der physik* **4** (1905).
- [2] R. V. Pound and G. A. Rebka. “Gravitational red-shift in nuclear resonance”. *Phys. Rev. Lett.* **3**, 439–441 (1959).
- [3] J. C. Hafele and R. E. Keating. “Around-the-world atomic clocks: Predicted relativistic time gains”. *Science* **177**, 166–168 (1972).
- [4] I. I. Shapiro. “Fourth test of general relativity”. *Phys. Rev. Lett.* **13**, 789–791 (1964).
- [5] I. I. Shapiro, M. E. Ash, R. P. Ingalls, W. B. Smith, D. B. Campbell, R. B. Dyce, R. F. Jurgens, and G. H. Pettengill. “Fourth test of general relativity: New radar result”. *Phys. Rev. Lett.* **26**, 1132–1135 (1971).
- [6] R. Colella, A. W. Overhauser, and S. A. Werner. “Observation of gravitationally induced quantum interference”. *Phys. Rev. Lett.* **34**, 1472–1474 (1975).
- [7] M. Kasevich and S. Chu. “Atomic interferometry using stimulated Raman transitions”. *Phys. Rev. Lett.* **67**, 181–184 (1991).
- [8] M. Kasevich and S. Chu. “Measurement of the gravitational acceleration of an atom with a light-pulse atom interferometer”. *Applied Physics B* **54**, 321–332 (1992).
- [9] A. Peters, K. Y. Chung, and S. Chu. “Measurement of gravitational acceleration by dropping atoms”. *Nature* **400**, 849–852 (1999).
- [10] J. M. McGuirk, G. T. Foster, J. B. Fixler, M. J. Snadden, and M. A. Kasevich. “Sensitive absolute-gravity gradiometry using atom interferometry”. *Phys. Rev. A* **65**, 033608 (2002).
- [11] J. B. Fixler, G. T. Foster, J. M. McGuirk, and M. A. Kasevich. “Atom interferometer measurement of the Newtonian constant of gravity”. *Science* **315**, 74–77 (2007).

[12] G. Lamporesi, A. Bertoldi, L. Cacciapuoti, M. Prevedelli, and G. M. Tino. “Determination of the Newtonian gravitational constant using atom interferometry”. *Phys. Rev. Lett.* **100**, 050801 (2008).

[13] G. Rosi, F. Sorrentino, L. Cacciapuoti, M. Prevedelli, and G. M. Tino. “Precision measurement of the Newtonian gravitational constant using cold atoms”. *Nature* **510**, 518 (2014).

[14] G. Rosi, L. Cacciapuoti, F. Sorrentino, M. Menchetti, M. Prevedelli, and G. M. Tino. “Measurement of the gravity-field curvature by atom interferometry”. *Phys. Rev. Lett.* **114**, 013001 (2015).

[15] T. Kovachy, P. Asenbaum, C. Overstreet, C. A. Donnelly, S. M. Dickerson, A. Sugarbaker, J. M. Hogan, and M. A. Kasevich. “Quantum superposition at the half-metre scale”. *Nature* **528**, 530–533 (2015).

[16] L. Hu, N. Poli, L. Salvi, and G. M. Tino. “Atom interferometry with the Sr optical clock transition”. *Phys. Rev. Lett.* **119**, 263601 (2017).

[17] P. Asenbaum, C. Overstreet, M. Kim, J. Curti, and M. A. Kasevich. “Atom-interferometric test of the equivalence principle at the 10^{-12} level”. *Phys. Rev. Lett.* **125**, 191101 (2020).

[18] R. Charrière, M. Cadoret, N. Zahzam, Y. Bidel, and A. Bresson. “Local gravity measurement with the combination of atom interferometry and Bloch oscillations”. *Phys. Rev. A* **85**, 013639 (2012).

[19] M. Andia, R. Jannin, F. Nez, F. Biraben, S. Guellati-Khélifa, and P. Cladé. “Compact atomic gravimeter based on a pulsed and accelerated optical lattice”. *Phys. Rev. A* **88**, 031605 (2013).

[20] X. Zhang, R. P. del Aguila, T. Mazzoni, N. Poli, and G. M. Tino. “Trapped-atom interferometer with ultracold Sr atoms”. *Phys. Rev. A* **94**, 043608 (2016).

[21] V. Xu, M. Jaffe, C. D. Panda, S. L. Kristensen, L. W. Clark, and H. Müller. “Probing gravity by holding atoms for 20 seconds”. *Science* **366**, 745–749 (2019).

[22] C. D. Panda, M. Tao, J. Egelhoff, M. Ceja, V. Xu, and H. Müller. “Coherence limits in lattice atom interferometry at the one-minute scale”. *Nature Physics* (2024).

[23] S. Sinha and J. Samuel. “Atom interferometry and the gravitational redshift”. *Classical and Quantum Gravity* **28**, 145018 (2011).

[24] M. Zych, F. Costa, I. Pikovski, and Č. Brukner. “Quantum interferometric visibility as a witness of general relativistic proper time”. *Nature Communications* **2** (2011).

[25] M. Zych, F. Costa, I. Pikovski, T. C. Ralph, and Č. Brukner. “General relativistic effects in quantum interference of photons”. *Classical and Quantum Gravity* **29**, 224010 (2012).

[26] E. Castro-Ruiz, F. Giacomini, and Č. Brukner. “Entanglement of quantum clocks through gravity”. *Proceedings of the National Academy of Sciences* **114**, E2303–E2309 (2017).

[27] S. Loriani et al. “Interference of clocks: A quantum twin paradox”. *Sci. Adv.* **5**, eaax8966 (2019).

[28] A. Roura. “Gravitational redshift in quantum-clock interferometry”. *Phys. Rev. X* **10**, 021014 (2020).

[29] E. Castro-Ruiz, F. Giacomini, A. Belenchia, and Č. Brukner. “Quantum clocks and the temporal localisability of events in the presence of gravitating quantum systems”. *Nat Commun* **11**, 2672 (2020).

[30] A. R. H. Smith and M. Ahmadi. “Quantum clocks observe classical and quantum time dilation”. *Nat. Commun.* **11**, 5360 (2020).

[31] S. Khandelwal, M. P. E. Lock, and M. P. Woods. “Universal quantum modifications to general relativistic time dilation in delocalised clocks”. *Quantum* **4**, 309 (2020).

[32] P. T. Grochowski, A. R. H. Smith, A. Dragan, and K. Dębski. “Quantum time dilation in atomic spectra”. *Phys. Rev. Res.* **3**, 023053 (2021).

[33] J. Paczos, K. Dębski, P. T. Grochowski, A. R. H. Smith, and A. Dragan. “Quantum time dilation in a gravitational field”. *Quantum* **8**, 1338 (2024).

[34] K. Dębski, P. T. Grochowski, R. Demkowicz-Dobrzański, and A. Dragan. “Universality of quantum time dilation”. *Classical and Quantum Gravity* **41**, 135014 (2024).

[35] P. A. Bushev, J. H. Cole, D. Sholokhov, N. Kukharchyk, and M. Zych. “Single electron relativistic clock interferometer”. *New Journal of Physics* **18**, 093050 (2016).

[36] A. Roura, C. Schubert, D. Schlippert, and E. M. Rasel. “Measuring gravitational time dilation with delocalized quantum superpositions”. *Phys. Rev. D* **104**, 084001 (2021).

[37] C. Ufrecht, F. Di Pumbo, A. Friedrich, A. Roura, C. Schubert, D. Schlippert, E. M. Rasel, W. P. Schleich, and E. Giese. “Atom-interferometric test of the universality of gravitational redshift and free fall”. *Phys. Rev. Res.* **2**, 043240 (2020).

[38] I. Meltzer and Y. Sagi. “Atomic clock interferometry using optical tweezers”. *Phys. Rev. A* **110**, 032602 (2024).

[39] M. Sonnleitner and S. M. Barnett. “Mass-energy and anomalous friction in quantum optics”. *Phys. Rev. A* **98**, 042106 (2018).

[40] M. Zych, Ł. Rudnicki, and I. Pikovski. “Gravitational mass of composite systems”. *Phys. Rev. D* **99**, 104029 (2019).

[41] P. K. Schwartz and D. Giulini. “Post-Newtonian corrections to Schrödinger equations in gravitational fields”. *Classical and Quantum Gravity* **36**, 095016 (2019).

[42] P. K. Schwartz and D. Giulini. “Post-Newtonian Hamiltonian description of an atom in a weak gravitational field”. *Phys. Rev. A* **100**, 052116 (2019).

[43] M. Zych. “Quantum systems under gravitational time dilation”. Springer Cham. (2017).

[44] M. Zych and Č. Brukner. “Quantum formulation of the Einstein equivalence principle”. *Nature Physics* **14**, 1027 (2018).

[45] F. Di Pumbo, C. Ufrecht, A. Friedrich, E. Giese, W. P. Schleich, and W. G. Unruh. “Gravitational redshift tests with atomic clocks and atom interferometers”. *PRX Quantum* **2**, 040333 (2021).

[46] D. E. Krause and I. Lee. “Relativistic coupling of internal and centre of mass dynamics in classical and simple bound quantum mechanical systems”. *Eur. J. Phys.* **38**, 045401 (2017).

[47] G. Tobar, S. Haine, F. Costa, and M. Zych. “Mass-energy equivalence in gravitationally bound quantum states of the neutron”. *Phys. Rev. A* **106**, 052801 (2022).

[48] V. Yudin and A. Taichenachev. “Mass defect effects in atomic clocks”. *Laser Physics Letters* **15**, 035703 (2018).

[49] R. Haustein, G. J. Milburn, and M. Zych. “Mass-energy equivalence in harmonically trapped particles” (2019). [arXiv:1906.03980](https://arxiv.org/abs/1906.03980).

[50] V. J. Martínez-Lahuerta, S. Eilers, T. E. Mehlstäubler, P. O. Schmidt, and K. Hammerer. “Ab initio quantum theory of mass defect and time dilation in trapped-ion optical clocks”. *Phys. Rev. A* **106**, 032803 (2022).

[51] A. Chu, V. J. Martínez-Lahuerta, M. Miklós, K. Kim, P. Zoller, K. Hammerer, J. Ye, and A. M. Rey. “Exploring the dynamical interplay between mass-energy equivalence, interactions, and entanglement in an optical lattice clock”. *Phys. Rev. Lett.* **134**, 093201 (2025).

[52] T. Bothwell et al. “Resolving the gravitational redshift across a millimetre-scale atomic sample”. *Nature* **602**, 420–424 (2022).

[53] X. Zheng, J. Dolde, V. Lochab, B. N. Merriman, H. Li, and S. Kolkowitz. “Differential clock comparisons with a multiplexed optical lattice clock”. *Nature* **602**, 425–430 (2022).

[54] R. H. Dicke. “The effect of collisions upon the doppler width of spectral lines”. *Phys. Rev.* **89**, 472–473 (1953).

[55] G. Grynberg. “Remarks on E1-E2 and E1-M1 two-photon transitions”. *Journal de Physique* **44**, 679–682 (1983).

[56] J. C. Bergquist, W. M. Itano, and D. J. Wineland. “Recoilless optical absorption and doppler sidebands of a single trapped ion”. *Phys. Rev. A* **36**, 428–430 (1987).

[57] Tetsuya Ido and Hidetoshi Katori. “Recoil-free spectroscopy of neutral sr atoms in the lamb-dicke regime”. *Phys. Rev. Lett.* **91**, 053001 (2003).

[58] H. Katori, M. Takamoto, V. G. Pal’chikov, and V. D. Ovsiannikov. “Ultrastable optical clock with neutral atoms in an engineered light shift trap”. *Phys. Rev. Lett.* **91**, 173005 (2003).

[59] E. A. Alden, K. R. Moore, and A. E. Leanhardt. “Two-photon E1-M1 optical clock”. *Phys. Rev. A* **90**, 012523 (2014).

[60] G. Janson, A. Friedrich, and R. Lopp. “Finite pulse-time effects in long-baseline quantum clock interferometry”. *AVS Quantum Science* **6** (2024).

[61] M. Cadoret et al. “Atom interferometry based on light pulses: Application to the

high precision measurement of the ratio h/m and the determination of the fine structure constant". *Eur. Phys. J. Spec. Top.* **172**, 121 (2009).

[62] P. Storey and C. Cohen-Tannoudji. "The Feynman path integral approach to atomic interferometry. A tutorial". *J. Phys. II France* **4**, 1999–2027 (1994).

[63] M. Werner, P. K. Schwartz, J. Kirsten-Siemß, N. Gaaloul, D. Giulini, and K. Hammerer. "Atom interferometers in weakly curved spacetimes using Bragg diffraction and Bloch oscillations". *Phys. Rev. D* **109**, 022008 (2024).

[64] R. B. Hutson, A. Goban, G. E. Marti, L. Sonderhouse, C. Sanner, and J. Ye. "Engineering quantum states of matter for atomic clocks in shallow optical lattices". *Phys. Rev. Lett.* **123**, 123401 (2019).

[65] X. Zheng, J. Dolde, M. C. Cambria, H. M. Lim, and S. Kolkowitz. "A lab-based test of the gravitational redshift with a miniature clock network". *Nat. Commun.* **14**, 4886 (2023).

[66] A. Aeppli, K. Kim, W. Warfield, M. S. Safronova, and J. Ye. "Clock with 8×10^{-19} systematic uncertainty". *Phys. Rev. Lett.* **133**, 023401 (2024).

[67] M. G. Tarallo, A. Alberti, N. Poli, M. L. Chiofalo, F.-Y. Wang, and G. M. Tino. "Delocalization-enhanced Bloch oscillations and driven resonant tunneling in optical lattices for precision force measurements". *Phys. Rev. A* **86**, 033615 (2012).

[68] F. Bloch. "Über die quantenmechanik der elektronen in kristallgittern". *Z. Physik* **52**, 555 (1929).

[69] C. Zener. "A theory of the electrical breakdown of solid dielectrics". *Proc. R. Soc. Lond. A* **145**, 523 (1934).

[70] A. P. Kolchenko, S. G. Rautian, and R. I. Sokolovskii. "Interaction of an atom with a strong electromagnetic field with the recoil effect taken into consideration". *Sov. Phys. JETP* **28**, 986 (1969).

[71] J. L. Hall, C. J. Bordé, and K. Uehara. "Direct optical resolution of the recoil effect using saturated absorption spectroscopy". *Phys. Rev. Lett.* **37**, 1339–1342 (1976).

[72] J. Ye, H. J. Kimble, and H. Katori. "Quantum state engineering and precision metrology using state-insensitive light traps". *Science* **320**, 1734–1738 (2008).

[73] G. H. Wannier. "Wave functions and effective hamiltonian for bloch electrons in an electric field". *Phys. Rev.* **117**, 432–439 (1960).

A Probability calculation

Here we derive the formula (1) for the probability $P_g^{(j)}$ of measuring the atom in the ground state in output $j \in \{0, 1\}$. We denote by $\Delta\phi$ the phase difference between upper and lower ground state trajectories, and by δ_d and δ_u the additional phase acquired by the excited state on the lower and upper trajectory, respectively. The final state of the atom $|\psi_{\text{final}}\rangle$ can be written in a generic way

$$|\psi_{\text{final}}\rangle = \frac{1}{8} |g\rangle \left(|0\rangle \left[1 - e^{i\delta_d} + e^{i\Delta\phi} \left(1 - e^{i\delta_u} \right) \right] - i |1\rangle \left[1 - e^{i\delta_d} - e^{i\Delta\phi} \left(1 - e^{i\delta_u} \right) \right] \right) + \dots, \quad (9)$$

where $|0\rangle$ and $|1\rangle$ are the states corresponding to two relevant output trajectories, and dots at the end stand for the parts of the state irrelevant to our considerations (lost trajectories and excited state). The factor $1/8 = (1/\sqrt{2})^6$ in front comes from six laser pulses applied to the atom (four Bragg pulses and two clock pulses). The minus signs in the bracket multiplying $|0\rangle$ result from the fact that excited state trajectories interacted with a laser two more times than the ground state trajectories (two clock pulses) — each interaction gives rise to the factor $i e^{i\phi_l}$ multiplying the corresponding trajectory (here ϕ_l is the so-called laser phase and we absorb it into phases $\Delta\phi$, δ_d , and δ_u). The factor $-i$ multiplying $|1\rangle$ reflects the fact that trajectories leaving the interferometer in output 1 interacted with the odd number of Bragg pulses (the lower trajectory interacted once, the upper one three times), while the ones leaving in output 0 interacted with the even number (two) of Bragg pulses. Finally, the additional minus sign in the bracket multiplying $|1\rangle$ comes from the fact that, in the case of trajectories leaving in output 1, the upper trajectory interacted with two more Bragg pulses than the lower one.

The amplitude of finding the atom in the ground state in the output j is given by

$$\langle g, j | \psi_{\text{final}} \rangle \propto \frac{1}{8} \left[1 - e^{i\delta_d} + (-1)^j e^{i\Delta\phi} \left(1 - e^{i\delta_u} \right) \right], \quad (10)$$

where we omitted the common phase factor $-i$ present in the case of $j = 1$. To calculate the probability $P_g^{(j)}$ we take the absolute value squared of the above amplitude and get

$$P_g^{(j)} = |\langle g, j | \psi_{\text{final}} \rangle|^2 = \frac{1}{16} \left[1 - \cos \left(\frac{\delta_u + \delta_d}{2} \right) \cos \left(\frac{\delta_u - \delta_d}{2} \right) + (-1)^j 2 \cos \left(\Delta\phi + \frac{\delta_u - \delta_d}{2} \right) \sin \left(\frac{\delta_d}{2} \right) \sin \left(\frac{\delta_u}{2} \right) \right], \quad (11)$$

which is exactly Eq. (1).

B Fall of the excited-state trajectory

Let us motivate the use of the perturbative method [62] by analyzing the fall of the excited-state trajectory during Bloch oscillations. We assume that the frequencies of the optical lattice lasers are chosen such that the ground state follows a bouncing trajectory at a fixed height (i.e., each interaction with the laser occurs at the same height z_B). Then, the excited-state trajectory necessarily falls with each bounce, due to its greater mass. Indeed, since we assume that the interaction with the laser occurs only when the atom reaches downward velocity $v_B = \hbar k/m$, and the momentum transferred to the atom in each interaction is the same for both the ground and the excited state, the excited state will move after each interaction with the upward velocity $v_B - \delta v_B$, where the velocity difference δv_B is given by

$$\delta v_B = 2v_B \frac{\delta m}{m}. \quad (12)$$

Since the velocity of the excited state right before each interaction is larger (in terms of the absolute value) than right after it, each subsequent interaction will occur lower by

$$\delta z_B = \frac{v_B \delta v_B}{g} \quad (13)$$

than the previous one meaning that the excited-state trajectory will progressively fall.

Also, the excited trajectory's smaller starting velocity means it will reach the downward velocity v_B faster than the ground state. Two subsequent interactions on the excited-state trajectory are separated by a time $\tau_B - \delta\tau_B$, where

$$\delta\tau_B = \frac{\delta v_B}{g}. \quad (14)$$

The spatial separation between the ground and the excited state trajectories is maximal when the excited state interacts with the laser. Then, it changes the direction of motion and meets the ground state trajectory at its interaction height z_B . Therefore, the trajectories meet repeatedly (at the interaction points of the ground state trajectory), but at each subsequent meeting point the excited-state trajectory has velocity lower by δv_B than at the previous meeting point (while the ground state moves there at velocity v_B).

The largest separation between the n th and $(n+1)$ th interaction on the ground state trajectory occurs at the moment of $(n+1)$ th interaction on the excited-state trajectory and is equal to $2n\delta z_B$. For the experimental parameters from [20] (strontium atoms, optical lattice operating at 532 nm, around 500 oscillations) the maximal separation between the ground and excited state trajectories would be around 10^{-13} m. This should be compared with the thermal wavelength of the atoms given by

$$\lambda_{\text{th}} = \sqrt{\frac{2\pi\hbar^2}{mk_B T}}, \quad (15)$$

where T is the temperature. In the experiment [20] the atoms were cooled to ~ 400 nK, corresponding to $\lambda_{\text{th}} \sim 10^{-7}$ m. Therefore, the thermal wavelength is much larger than the separation between the trajectories, and it is justified to use the perturbative approach in phase calculations.

C Phases

Let us calculate the phases $\Delta\phi$, δ_d , and δ_u using the perturbative method developed in [62]. Each consists of two contributions: the propagation phase calculated by integrating the free-fall Lagrangian over the trajectory followed by the atom, and the laser phase resulting from atom-light interactions.

The free-fall Lagrangian of a relativistic particle with the internal two-level structure incorporating the mass-energy equivalence can be expanded to the order $1/c^2$ as follows:

$$L = -\hat{m}c^2 - \hat{m}\left(gz - \frac{1}{2}v^2\right) - \frac{\hat{m}}{c^2}\left(\frac{1}{2}g^2z^2 - \frac{1}{8}v^4 + \frac{3}{2}gzbv^2\right) + \mathcal{O}\left(\frac{1}{c^4}\right). \quad (16)$$

Here \hat{m} is the mass operator returning m for the ground state, and $m + \delta m$ (where $\delta m = \hbar\omega_0/c^2$) for the excited state of the atom. At this point, we distinguish the $1/c^2$ correction to the excited-state Lagrangian coming from the mass-energy equivalence

$$\delta L^{(1)} = -\delta m\left(gz - v^2/2\right), \quad (17)$$

and the correction to the (ground- and excited-state) Lagrangian coming from the expansion of the relativistic-particle Lagrangian up to $1/c^2$ order

$$\delta L^{(2)} = -\frac{m}{c^2}\left(\frac{1}{2}g^2z^2 - \frac{1}{8}v^4 + \frac{3}{2}gzbv^2\right). \quad (18)$$

Here we replaced \hat{m} by m because δm is of the order $1/c^2$ and would contribute in higher order to the above expression. Note that for the scenario considered in this work, based on numbers from [20], $\delta L^{(2)} \ll \delta L^{(1)}$. This is because the internal energy of the atomic transition (~ 1 eV) is much larger than the kinetic energy of the atom or the gravitational energy difference between the trajectories (both $\sim 10^{-10}$ eV).

Note also that the correction $\delta L^{(2)}$ and the corrections to the laser phases derived in [63] depend only on the trajectory, not on the internal state. Therefore, in the picture in which both the ground and the excited state follow the same trajectory, they will contribute only to the phase $\Delta\phi$, not to δ_d and δ_u . We are not interested in $1/c^2$ corrections to $\Delta\phi$, hence we will omit them in the subsequent analysis and focus only on the corrections coming from $\delta L^{(1)}$.

We begin with the calculation of $\Delta\phi$. To calculate the propagation phase contribution we divide the trajectory into freely falling pieces between points of interaction with the lasers and calculate the propagation phase by integrating the freely falling Lagrangian

$$L_g = -m\left(c^2 + gz - v^2/2\right) \quad (19)$$

along the trajectory. More precisely, for the free fall starting at time t_A and ending at t_B , the propagation phase is given by

$$\begin{aligned} \phi_p(t_A \rightarrow t_B) &= \frac{1}{\hbar} \int_{t_A}^{t_B} dt L_g = -\frac{m}{\hbar} \int_{t_A}^{t_B} dt \left(c^2 + gz - v^2/2\right) \\ &= -\frac{m}{\hbar} \left[\left(c^2 + g z_A - \frac{1}{2}v_A^2\right) (t_B - t_A) + v_A g (t_B - t_A)^2 - \frac{1}{3}g^2(t_B - t_A)^3 \right], \end{aligned} \quad (20)$$

where z_A and v_A are the atom's position and velocity, respectively, at time t_A . Denote by t_j with $j \in \{1, 2, 3, 4\}$ the times at which consecutive Bragg pulses are applied, and by t_i and t_f the times of the initial and final clock pulses, respectively. Notice that to match the notation from the main text, the times of application of particular pulses must satisfy

$$t_2 - t_1 = t_4 - t_3 = T, \quad t_i - t_2 = t_3 - t_f = T', \quad t_f - t_i = T_B. \quad (21)$$

Let us further denote the quantities corresponding to the lower and upper trajectories by superscripts (d) and (u), respectively, and by $\Delta\phi_p(t_A \rightarrow t_B) = \phi_p^{(u)}(t_A \rightarrow t_B) - \phi_p^{(d)}(t_A \rightarrow t_B)$ the propagation phase difference between those two trajectories acquired between t_A and t_B . Let us consider one by one the consecutive stages of the interferometer and calculate the corresponding phase difference using (20).

- $t_1 \rightarrow t_2$:

At time t_1 both trajectories are at the same height, but the upper one starts with a velocity greater by Δv than the lower one. Denote the initial velocity of the lower trajectory by v_1 . Then, the relative propagation phase acquired between t_1 and t_2 reads

$$\Delta\phi_p(t_1 \rightarrow t_2) = \frac{m}{\hbar} \Delta v T \left(v_1 + \frac{1}{2} \Delta v - gT \right). \quad (22)$$

- $t_2 \rightarrow t_i$:

Both trajectories start with the same velocity, but the upper one is higher by $\Delta v T$. The relative propagation phase is given by

$$\Delta\phi_p(t_2 \rightarrow t_i) = -\frac{m}{\hbar} g \Delta v T T'. \quad (23)$$

- $t_i \rightarrow t_f$:

We assume that both trajectories oscillate with the same frequency, and start simultaneously with zero initial velocity and maximal height. Therefore, the trajectories are constantly separated by $\Delta v T$ and have the same velocities all the time. The relative propagation phase equals

$$\Delta\phi_p(t_i \rightarrow t_f) = -\frac{m}{\hbar} g \Delta v T T_B. \quad (24)$$

- $t_f \rightarrow t_3$:

Similar to the previous two points, the velocity on both trajectories is the same, and they are separated by $\Delta v T$. The propagation phase difference reads

$$\Delta\phi_p(t_f \rightarrow t_3) = -\frac{m}{\hbar} g \Delta v T T'. \quad (25)$$

- $t_3 \rightarrow t_4$:

The trajectories start separated by $\Delta v T$, and the upper one has a velocity smaller by Δv . Denote the initial velocity of the lower trajectory by v_3 . The relative propagation phase is then given by

$$\Delta\phi_p(t_3 \rightarrow t_4) = \frac{m}{\hbar} \Delta v T \left(-v_3 + \frac{1}{2} \Delta v \right). \quad (26)$$

To calculate the total propagation phase difference $\Delta\phi_p$ we sum up all the contributions, which gives

$$\Delta\phi_p = \frac{m}{\hbar} \Delta v T [v_1 + \Delta v - v_3 - g(T + 2T' + T_B)]. \quad (27)$$

Finally, let us note that, because of the requirement that at t_i the velocity on both trajectories is equal to zero, the following relation holds

$$v_1 + \Delta v = g(T + T'). \quad (28)$$

On the other hand, v_3 is the velocity that the atom reaches after time T' of a free fall after leaving the optical lattice. Let us notice that the atom does not leave the optical lattice with zero velocity (see Fig. 2), but rather with velocity $-g\tau$. Here $\tau \in \{-\tau_B/2, \tau_B/2\}$ is given by

$$T_B = N\tau_B + \tau, \quad (29)$$

where $N = \lfloor T_B/\tau_B + 1/2 \rfloor$ is the number of interactions between the optical lattice and the atom. Therefore, we have

$$v_3 = -g(\tau + T') \quad (30)$$

and we can rewrite Eq. (27) (introducing $\Delta z = \Delta v T$) as follows:

$$\Delta\phi_p = \frac{m}{\hbar} \Delta z g(\tau - T_B) = -\frac{m}{\hbar} g \Delta z N \tau_B. \quad (31)$$

Now, let us focus on the laser phase contribution to the phase $\Delta\phi$. As described in [62], when the atom absorbs (emits) a photon with frequency ω and wave vector k , it acquires a laser phase

$$\phi_l(t, z) = \mp\omega t \pm kz, \quad (32)$$

where the upper (lower) sign corresponds to photon absorption (emission), and t and z are the time and position of the interaction, respectively. In the case of Bragg pulses, as well as in the optical lattice, the photon absorption is immediately followed by the emission of a photon with the same frequency and opposite wave vector. Therefore, the laser phase acquired at each such interaction point is equal to $\phi_l(t, z) = \phi_l(z) = \pm 2kz$ with the plus (minus) sign corresponding to the atom receiving upward (downward) momentum.

Denote by z_j with $j \in \{1, 2, 3, 4\}$ the interaction heights with four consecutive Bragg pulses (z_1 and z_3 correspond to the upper trajectory, while z_2 and z_4 to the lower one), and by z_d and z_u the heights of interactions of the lower and upper trajectories, respectively, within the optical lattice. Note also that the wave vector k_{Bragg} of the pulses is related to the velocity change Δv by

$$2\hbar k_{\text{Bragg}} = m\Delta v, \quad \Rightarrow \quad k_{\text{Bragg}} = \frac{m\Delta v}{2\hbar}, \quad (33)$$

and the wave vector k_{Bloch} of the optical lattice laser is related to the Bloch period τ_B by

$$2\hbar k_{\text{Bloch}} = mg\tau_B, \quad \Rightarrow \quad k_{\text{Bloch}} = \frac{mg\tau_B}{2\hbar}. \quad (34)$$

The total laser phase difference (between the upper and lower trajectory) is given by

$$\Delta\phi_l = 2k_{\text{Bragg}}(z_1 - z_2 - z_3 + z_4) + 2Nk_{\text{Bloch}}(z_u - z_d) \quad (35)$$

Let us notice the following relations between particular heights:

$$z_2 - z_1 = v_1 T - \frac{1}{2}gT^2, \quad z_4 - z_3 = (v_3 - \Delta v)T - \frac{1}{2}gT^2, \quad z_u - z_d = \Delta z, \quad (36)$$

where v_1 and v_3 are given by (28) and (30). Hence, we can write the total laser phase difference as

$$\Delta\phi_l = \frac{m}{\hbar} [-g\Delta z(T + 2T' + \tau) + g\Delta z N\tau_B]. \quad (37)$$

The total phase difference $\Delta\phi$ between the upper and the lower (ground state) trajectories is calculated by summing up the total propagation phase difference and the total laser phase difference. This gives

$$\Delta\phi = \Delta\phi_p + \Delta\phi_l = -\frac{mg\Delta z}{\hbar}(T + 2T' + \tau). \quad (38)$$

Now, let us calculate the additional phases δ_d and δ_u acquired by the excited state on the lower and upper trajectory, respectively. We need to calculate the additional laser phase coming from the clock pulses and the correction to the propagation phase due to the mass-energy equivalence. Starting with the laser phase, we assume that the clock pulses change only the atom's internal state, but do not affect its motion. This can be achieved by driving two-photon transitions with both photons having the same frequency $\omega/2$ and opposite momenta. The corresponding laser phase is equal to $\mp\omega t$ with the minus (plus) sign corresponding to the two-photon absorption (emission). Note that this phase is independent of the position z of the interaction (thus, it is the same for the lower and upper trajectory). Since the excited state trajectories absorb the photons at t_i and emit at t_f , they acquire the laser phase $\omega(t_f - t_i) = \omega T_B$.

To calculate the propagation phase correction, we employ the perturbative method developed in [62] and integrate the mass-energy correction to the free-fall Lagrangian

$$\delta L = -\delta m \left(c^2 + gz - v^2/2 \right) \quad (39)$$

over the ground state trajectory on the corresponding height. For the free-fall trajectory starting at t_a and ending at t_B the correction $\delta_p(t_a \rightarrow t_B)$ to the propagation phase reads (compare with (20))

$$\delta_p(t_a \rightarrow t_B) = -\frac{\delta m}{\hbar} \left[\left(c^2 + gz_a - \frac{1}{2}v_a^2 \right) (t_B - t_a) + v_a g (t_B - t_a)^2 - \frac{1}{3}g^2 (t_B - t_a)^3 \right]. \quad (40)$$

For a full single oscillation in the optical lattice starting at height z_B with velocity v_B , the propagation phase correction $\delta_{p,1}$ is given by

$$\delta_{p,1} = \frac{\delta m}{\hbar} \left[-c^2 - g \left(z_B + \frac{v_B^2}{3} \right) + \frac{v_B^2}{6} \right] \tau_B \equiv -\omega_0 \tau_B \left[1 + \frac{g\langle z \rangle}{c^2} - \frac{\langle v^2 \rangle}{2c^2} \right], \quad (41)$$

where τ_B is the oscillation period, we have used the fact that $\delta m = \hbar\omega_0/c^2$, and introduced $\langle z \rangle$ and $\langle v^2 \rangle$ for the mean height and velocity squared. We assume that the total number N of Bloch oscillations is large, and neglect the correction coming from the fact that the total time T_B of Bloch oscillations is not necessarily equal to the integer multiple of Bloch periods (instead, $T_B = N\tau_B + \tau$ with $\tau \in (-\tau_B/2, \tau_B/2)$; however, since $\tau \ll N\tau_B$, we will assume $\tau \approx 0$). Then, the total propagation phase correction is given by

$$\delta_{p,\text{tot}} \approx N\delta_{p,1} = -\omega_0 N \tau_B \left[1 + \frac{g\langle z \rangle}{c^2} - \frac{\langle v^2 \rangle}{2c^2} \right] \approx -\omega_0 T_B \left[1 + \frac{g\langle z \rangle}{c^2} - \frac{\langle v^2 \rangle}{2c^2} \right]. \quad (42)$$

Without loss of generality, we can assume that the mean height corresponding to the lower trajectory $\langle z \rangle_d = 0$, while this of the upper one equals $\langle z \rangle_u = \Delta z$. Combining the propagation phase with the laser phase corrections, we get

$$\begin{aligned} \delta_d &= \left[\omega - \omega_0 \left(1 - \frac{\langle v^2 \rangle}{2c^2} \right) \right] T_B, \\ \delta_u &= \left[\omega - \omega_0 \left(1 + \frac{g\Delta z}{c^2} - \frac{\langle v^2 \rangle}{2c^2} \right) \right] T_B. \end{aligned} \quad (43)$$

D Non-perturbative calculations

As a consistency check let us compute the phases accumulated during the Bloch oscillations non-perturbatively, namely for the trajectories described in Appendix B, and make sure that they agree with the perturbative calculation from Appendix C. In the following, we restrict all the calculations to the terms up to order $1/c^2$ neglecting the higher-order terms. This is consistent with the perturbative approach, where we considered only $1/c^2$ corrections.

Since the trajectories of the ground and excited states no longer coincide (the excited trajectory falls), the phase difference between them will gain contribution from three different sources: the propagation phase, the laser phase, and the separation phase. The first two are defined in the same way as in the previous (perturbative) considerations, and the third one is given by

$$\delta_s(t) \equiv \frac{\bar{p}(t)\Delta z(t)}{\hbar}, \quad (44)$$

where $\bar{p}(t)$ is the mean momentum of two trajectories at time t (the oscillation starts at $t = 0$), and $\Delta z(t)$ is the separation between them (note that this has nothing to do with the separation Δz between the upper and lower trajectory).

Since the phase acquired due to the interaction with the clock pulses is position-independent, it will not change in the non-perturbative analysis. Therefore, we consider only the phases acquired during the Bloch oscillations within the optical lattice. The trajectory followed by both trajectories has been described above. We analyze only the time between the two first interactions on the ground state

trajectory (at some arbitrary height z_B) and show that the phase difference between the ground and the excited state trajectories agrees with the perturbative calculations. It is straightforward that it will agree with the perturbative calculations also at later times.

The propagation phases acquired on both trajectories in the first part of the oscillation (before the second interaction of the excited state) can be calculated using the general formula for the propagation phase in free fall:

$$\phi_p^{(g/e)}(t) = \frac{m^{(g/e)}}{\hbar} \left[\left(-c^2 + \frac{1}{2}v_0^2 - gz_0 \right) t - v_0 gt^2 + \frac{1}{3}g^2 t^3 \right], \quad (45)$$

(this is just Eq. (20) with $t_A \rightarrow 0$ and $t_B \rightarrow t$) where $m^{(g)} = m$ and $m^{(e)} = m + \delta m$ are the masses of the atom in the ground and excited state, respectively, v_0 is the initial velocity, and z_0 is the initial height. For the ground state, we replace v_0 by v_B , while for the excited state by $v_B - \delta v_B$. The initial height for both states is the same and equal to z_B .

The difference in propagation phases at time t is then given by

$$\delta_p(t) = \phi_p^{(e)}(t) - \phi_p^{(g)}(t) = \frac{\delta m}{\hbar} \left[\left(-c^2 + \frac{1}{2}v_B^2 - gz_B \right) t - v_B gt^2 + \frac{1}{3}g^2 t^3 \right] - \frac{m}{\hbar} (v_B - gt) \delta v_B t \quad (46)$$

(recall that we neglect the terms higher-order than $1/c^2$). Let us notice that, since $\delta v_B t$ is just the separation $\Delta z(t)$ between the trajectories, the second term in the above formula is equal in value but with the opposite sign to the separation phase

$$\delta_s(t) = \frac{\bar{p}(t) \delta v_B t}{\hbar} = \frac{m}{\hbar} (v_B - gt) \delta v_B t, \quad (47)$$

where $\bar{p}(t) = m(v_B - gt) + \mathcal{O}(1/c^2)$. Therefore, the total phase difference for $t < \tau_B - \delta v_B/g$ is given by

$$\delta_p(t) + \delta_s(t) = \frac{\delta m}{\hbar} \left[\left(-c^2 + \frac{1}{2}v_B^2 - gz_B \right) t - v_B gt^2 + \frac{1}{3}g^2 t^3 \right], \quad (48)$$

in agreement with the perturbative results (indeed, this is just the propagation phase correction calculated in the perturbative approach).

At the time $\tau_B - \delta v_B/g$ the interaction of the atom on the excited trajectory with the laser occurs, and it acquires a laser phase

$$\phi_l^{(e)} = \frac{m}{\hbar} 2v_B(z_B - \delta z_B) = \phi_l^{(g)} - \frac{m}{\hbar} \delta v_B \tau_B + \mathcal{O}(\delta m^2), \quad (49)$$

where $\phi_l^{(g)}$ is the laser phase acquired by the ground state trajectory at time τ_B . Let us notice that right before the second interaction of the excited state the separation phase is equal to

$$\delta_s(\tau_B - \Delta v/g - \varepsilon) = -\frac{m}{\hbar} v_B \delta v_B t, \quad (50)$$

while right after the interaction it is $\sim \mathcal{O}(1/c^4)$, because the mean momentum is then $\sim \mathcal{O}(1/c^2)$. This situation (mean momentum $\sim \mathcal{O}(1/c^2)$ and thus negligible value of the separation phase) persists until the second interaction on the ground state trajectory, at which time both trajectories are at the same height, but the excited one has the velocity $v_B - 2\delta v_B$. At this point, we can repeat the entire analysis changing everywhere $\delta v_B \rightarrow 2\delta v_B$. Since the propagation phase difference acquired between the second interaction on the excited and on the ground trajectories is also $\sim \mathcal{O}(\delta m^2)$, the total phase difference after the first oscillation is equal to

$$\delta = \delta_p + \delta_s + \delta_l = \frac{\delta m}{\hbar} \left[\left(-c^2 + \frac{1}{2}v_B^2 - gz_B \right) \tau_B - v_B g \tau_B^2 + \frac{1}{3}g^2 \tau_B^3 \right] = \frac{\delta m}{\hbar} \left[-c^2 - g \left(z_B + \frac{v_B^2}{3} \right) + \frac{v_B^2}{6} \right] \tau_B, \quad (51)$$

which is equal to the propagation phase correction calculated for a single oscillation in the perturbative approach (compare with Eq. (41)).

E Bloch oscillations — the usual description

In our analysis, we have employed a simplified model of Bloch oscillations based on [19, 61], where the oscillating atom follows a bouncing trajectory in a gravitational field (see Fig. 2). However, this is not the most common description of Bloch oscillations — usually one assumes that the dynamics of the atom is set by a periodic potential (optical lattice) and a linear correction (gravitational field), which leads to the oscillatory motion [68, 69]. The full Hamiltonian of the system involving the leading relativistic corrections reads

$$\hat{H} = mc^2 + \frac{\hat{p}^2}{2m} + mg\hat{z} + V_0 \cos(2k_{\text{Bloch}}\hat{z}) + \hbar\omega_0 |e\rangle\langle e| \left(1 + \frac{g\hat{z}}{c^2} - \frac{\hat{p}^2}{2m^2c^2} \right) \equiv \hat{H}^{(0)} + \hat{H}^{(1)}, \quad (52)$$

where V_0 is the depth of the optical lattice potential, k_{Bloch} is the wave vector of the lattice photons, $|e\rangle\langle e|$ is a projector on the excited state of the atom, and

$$\begin{aligned} \hat{H}^{(0)} &= \hat{H}_{\text{cm}}^{(0)} + \hat{H}_{\text{int}}^{(0)}, \\ \hat{H}_{\text{cm}}^{(0)} &= \frac{\hat{p}^2}{2m} + mg\hat{z} + V_0 \cos(2k_{\text{Bloch}}\hat{z}), \\ \hat{H}_{\text{int}}^{(0)} &= mc^2 + \hbar\omega_0 |e\rangle\langle e|, \\ \hat{H}^{(1)} &= \frac{\hbar\omega_0}{c^2} |e\rangle\langle e| \left(g\hat{z} - \frac{\hat{p}^2}{2m^2} \right). \end{aligned} \quad (53)$$

Writing Eq. (52) we have assumed that the lattice operates at the “magic” wavelength [58, 72], which means that the harmonic potential experienced by the ground and excited state atoms is the same. Let us notice that the frequency of the light as perceived by the atom depends on its position and velocity (due to the relativistic Doppler shifts). Therefore, in principle, it can only be at the “magic” wavelength for an atom at some specific height and velocity. The atom at some other height, or moving with a different velocity, will perceive the light as shifted from this wavelength, leading to a dependence of the optical lattice potential on the center-of-mass degrees of freedom. Note that this is exactly analogous to the situation in optical lattice clocks, where the atoms are not perfectly static and are placed at different heights. However, it was shown in [58] that around the “magic” wavelength the potential changes very slowly with the frequency of the lattice laser, and the corrections due to Doppler shifts can be made negligible. Consequently, we shall omit them from further consideration.

To calculate the phase shifts in the Hamiltonian formalism we use the time-independent perturbation theory. We treat the Hamiltonian $\hat{H}^{(1)}$ in Eq. (52) as a small correction to $\hat{H}^{(0)}$. The eigenstates of $\hat{H}^{(0)}$ belong to the Hilbert space $\mathcal{H}_{\text{cm}} \otimes \mathcal{H}_{\text{int}}$ with \mathcal{H}_{cm} spanned by the Wannier-Stark states [73], and \mathcal{H}_{int} by $\{|g\rangle, |e\rangle\}$. We assume that the center-of-mass state (the part corresponding to \mathcal{H}_{cm}) is the same for both internal states of the atom. In the zeroth order, the phase shift is equal on both trajectories (lower and upper) and reads

$$\delta_{\text{d}}^{(0)} = \delta_{\text{u}}^{(0)} = (\omega - \omega_0)T_{\text{B}}. \quad (54)$$

The first-order (in $1/c^2$) correction to the phases results from the correction to the eigenenergies and is given by

$$\delta_i^{(1)} = -\frac{1}{\hbar} \left(\langle \hat{H}^{(1)} \rangle_{e,i} - \langle \hat{H}^{(1)} \rangle_{g,i} \right) T_{\text{B}}, \quad (55)$$

where the expectation values are evaluated on unperturbed states. In the ground state, the expectation value of $\hat{H}^{(1)}$ is zero irrespectively of the path, and in the excited state we have

$$\langle \hat{H}^{(1)} \rangle_{e,i} = \frac{\hbar\omega_0}{c^2} \left(g\langle \hat{z} \rangle_i - \frac{\langle \hat{p}^2 \rangle_i}{2m^2} \right). \quad (56)$$

This leads to the total phase shift of the form:

$$\delta_i = \delta_i^{(0)} + \delta_i^{(1)} = \left[\omega - \omega_0 \left(1 + \frac{g\langle \hat{z} \rangle_i}{c^2} - \frac{\langle \hat{p}^2 \rangle_i}{2m^2c^2} \right) \right] T_B, \quad (57)$$

which, upon identifications $\langle \hat{z} \rangle_i$ and $\langle \hat{p}^2 \rangle_i = m^2 \langle v^2 \rangle_i$, takes the same form as derived in Appendix C. Note the different meaning of the brackets in (57) and those present e.g. in (43) — in the first case they indicate averaging over the quantum state, while in the latter they mean taking the average over the classical trajectory.

The same results can be derived in the Lagrangian formalism using the method developed in [62]. We assume that the atom follows a superposition of classical trajectories set by the (ground-state) Lagrangian

$$L_g = -mc^2 + \frac{1}{2}mv^2 - mgz - V_0 \cos(2k_{\text{Bloch}}z), \quad (58)$$

corresponding to the Hamiltonian (52). Let us consider (following the reasoning from Appendix C) the dominant correction to the Lagrangian of the excited state atoms, i.e.,

$$\delta L = -\delta m \left(c^2 + gz - v^2/2 \right). \quad (59)$$

To calculate the phases δ_d and δ_u ($\Delta\phi$ does not depend on the model of Bloch oscillations that we use) we integrate the Lagrangian correction δL over the trajectory $z(t)$ followed by the atom (assuming that the trajectory is the same for both internal states). This gives (recall that $\delta m = \hbar\omega_0/c^2$)

$$\frac{1}{\hbar} \int_0^{T_B} dt \delta L = -\omega_0 T_B \left[1 + \frac{g}{c^2} \left(\frac{1}{T_B} \int_0^{T_B} dt z(t) \right) - \frac{1}{2c^2} \left(\frac{1}{T_B} \int_0^{T_B} dt v^2(t) \right) \right] \equiv -\omega_0 T_B \left[1 + \frac{g\langle z \rangle}{c^2} - \frac{\langle v^2 \rangle}{2c^2} \right], \quad (60)$$

where we have introduced

$$\langle z \rangle \equiv \frac{1}{T_B} \int_0^{T_B} dt z(t), \quad \langle v^2 \rangle \equiv \frac{1}{T_B} \int_0^{T_B} dt v^2(t). \quad (61)$$

Assuming that the mean height of the lower trajectory is set to zero and that of the upper one to Δz , that the mean squared velocity is the same on both heights and adding a laser phase ωT_B coming from the interaction with the clock pulse, we get

$$\begin{aligned} \delta_d &= \left[\omega - \omega_0 \left(1 - \frac{\langle v^2 \rangle}{2c^2} \right) \right] T_B, \\ \delta_u &= \left[\omega - \omega_0 \left(1 + \frac{g\Delta z}{c^2} - \frac{\langle v^2 \rangle}{2c^2} \right) \right] T_B, \end{aligned} \quad (62)$$

which is the same as derived in Appendix C. It is worth noting that the method developed in [62] was derived for quadratic Lagrangians, while Lagrangian (58) is nonquadratic. However, the compatibility with the result obtained in the Hamiltonian formalism suggests that the method from [62] is still applicable in our case.